Investigation of the Postcure Reaction and Surface Energy of Epoxy Resins Using Time-of-Flight Secondary Ion Mass Spectrometry and Contact-Angle Measurements

Firas Awaja,[1] Michael Gilbert,[3] Bronwyn Fox,[2] Georgina Kelly,[2] Paul J. Pigram[3]

[1]*School of Physics, University of Sydney, NSW 2006, Sydney, Australia*
[2]*Centre for Material and Fibre Innovation, Geelong Technology Precinct, Deakin University, Geelong, Victoria 3217, Australia*
[3]*Centre for Materials and Surface Science and Department of Physics, La Trobe University, Victoria 3086, Australia*

Received 16 July 2008; accepted 9 November 2008
DOI 10.1002/app.30135
Published online 29 April 2009 in Wiley InterScience (www.interscience.wiley.com).

ABSTRACT: Time-of-flight secondary ion mass spectrometry (ToF-SIMS) was used to investigate correlations between the molecular changes and postcuring reaction on the surface of a diglycidyl ether of bisphenol A and diglycidyl ether of bisphenol F based epoxy resin cured with two different amine-based hardeners. The aim of this work was to present a proof of concept that ToF-SIMS has the ability to provide information regarding the reaction steps, path, and mechanism for organic reactions in general and for epoxy resin curing and postcuring reactions in particular. Contact-angle measurements were taken for the cured and postcured epoxy resins to correlate changes in the surface energy with the molecular structure of the surface. Principal components analysis (PCA) of the ToF-SIMS positive spectra explained the variance in the molecular information, which was related to the resin curing and postcuring reactions with different hardeners and to the surface energy values. The first principal component captured information related to the chemical phenomena of the curing reaction path, branching, and network density based on changes in the relative ion density of the aliphatic hydrocarbon and the $C_7H_7O^+$ positive ions. The second principal component captured information related to the difference in the surface energy, which was correlated to the difference in the relative intensity of the $C_xH_yN_z^+$ ions of the samples. PCA of the negative spectra provided insight into the extent of consumption of the hardener molecules in the curing and postcuring reactions of both systems based on the relative ion intensity of the nitrogen-containing negative ions and showed molecular correlations with the sample surface energy. © 2009 Wiley Periodicals, Inc. J Appl Polym Sci 113: 2755–2764, 2009

Key words: adhesion; resins; surfaces

INTRODUCTION

Epoxy resins are flexible materials that can be formulated to fit the design of many structural applications.[1–3] Tailoring the properties of a cured epoxy resin for a specific application requires a thorough understanding of the chemistry of the curing and postcuring reactions.[3] These are affected by the processing conditions and the chemistry of the resin and the curing agent. A complex molecular network is generated as a result of the reactions between the resin and curing agent, and its molecular characteristics directly influence the end-product performance.[4,5] Investigations on the molecular level are essential to reveal the curing reaction pathways and to shed light on the structural arrangement of the resulting network. Curing reactions occurring at the surface are of particular importance because of their influence on properties such as the surface energy and, in turn, the adhesion strength of the product.[6]

Polymer surface energy is explored via surface tension; there are two approaches in common use. First is the components approach, in which the surface tension is considered to be a combination of dispersion forces (van der Waals forces) and polar forces (hydrogen bonding). Surface free energy models employed for interpreting results include those by Fowkes and by Owens, Wendt, Rabel, and Kaelble (geometric mean) and the Wu harmonic mean theory.[7,8] The second approach is an equation-of-state formula and is reported so that the surface energy can be calculated with only one contact-angle measurement.[9–12] There has been previous research on the correlation between the surface properties and molecular characteristics of epoxy and phenolic resins.[6,13–16] The surface polarity as a result of the presence of different functional groups is related to the overall surface energy.[13] Lim et al.[13] reported that an increase in surface hydrophilic properties after the plasma treatment of a glass-fiber epoxy resin composite resulted from changes in the surface

Correspondence to: F. Awaja (firas@physics.usyd.edu.au).

composition and specifically from a decrease in the relative concentration of carbon and an increase in the relative concentration of oxygen on the surface as measured by X-ray photoelectron spectroscopy. They explained that the high oxygen content on the surface was a result of the increased presence of carbonyl groups originating from reactions at the treated surface with oxygen and oxygen-containing molecules from the surrounding air. Lee et al.[6] showed that surface energies calculated with acid–base theory slightly decreased as a result of the progress of the curing reaction of the phenolic resol resin. They explained that this decrease in surface energy was due to the decrease in the number of hydroxyl groups at the surface and the molecular characteristics of the resol resin. Abbasian et al.[16] showed by the harmonic mean approach that the surface free energy did not change significantly as a result of the thickness of the polymer film used for contact-angle measurements. More information is needed to relate the superficial curing and postcuring reaction behavior of epoxy resins with the surface energy.

Time-of-flight secondary ion mass spectrometry (ToF-SIMS) has been used previously to provide insight into the curing and postcuring reactions of diglycidyl ether of bisphenol A (DGEBA)/isophorone diamine (IPD) hardeners under different conditions.[17,18] Awaja et al.[17] showed with a real-time monitoring system using ToF-SIMS that three reaction pathways were generated; these were monitored over a curing time of 24 h. It was found, through the changes in the intensity of the aliphatic hydrocarbon ions, that coupling and branching reactions occurred much faster than crosslinking and blocking reactions in the initial stage of the reaction. The changes in the relative intensities of the $C_{21}H_{24}O_4^+$, $C_{14}H_7O^+$, and $C_7H_7O^+$ ions provided a measure of the total conversion of the curing reaction at any given reaction time. Furthermore, it was shown that at different resin/hardener ratios,[18] the changes in the relative ion intensity of the $C_xH_yN_z^+$ ions were indicative of the unreacted and partially reacted hardener molecules and were proportional to the hardener concentration. The relative ion intensity of the listed aliphatic hydrocarbon ions was related to the crosslinking density of the epoxy resin.

Principal components analysis (PCA) is used to simplify often complex ToF-SIMS data. PCA has been used previously by many researchers in combination with ToF-SIMS to aid in the interpretation of polymer reactions on the molecular level.[19–21] The data that are collected in ToF-SIMS experiments are normally pretreated before the application of PCA. Data pretreatments, such as scaling and mean centering, ensure that the variance in the measured values is due to chemical differences between samples and not an artifact of variations in the total secondary ion current or detector efficiency.[20,21]

This study was designed to suggest a mechanism for curing and postcuring reactions for different hardener systems by explaining molecular changes at the surface of cured and postcured epoxy resins with ToF-SIMS and PCA. Contact-angle measurements were used to determine resulting changes in the surface energies and adhesion strength accompanying these molecular changes.

EXPERIMENTAL

Materials

The epoxy resin Kinetix R246TX (ATL Composites Southport, Queensland, Australia) was used in this study. The resin consists mainly of DGEBA blended with diglycidyl ether of bisphenol F (DGEBF) and aliphatic glycidyl ether as a functional diluent. A superfast hardener (Kinetix H126, ATL Composites), denoted in this study as hardener H, was employed. It is intended to induce curing at room temperature and has IPD as the main ingredient. The curing agent Ancamine 1637 (Air Products and Chemicals, Inc., United States), denoted in this study as hardener A, is a rapid Mannich–Base curing agent with a fast thin-film set time even under adverse, humid conditions. The ingredients of Ancamine 1637 include triethylene tetramine (Teta) and its reaction products with phenol/formaldehyde. Figure 1 shows the structures of the DGEBA, IPD, and Teta molecules. The sample naming convention used in this study includes the hardener type, the resin-to-hardener ratio, and the cured (C) or postcured (P) condition. For example, sample H3C was made with hardener type H with a resin-to-hardener ratio of 3 : 1, and it was cured but not postcured. Sample A4P was made with hardener type A with a resin-to-hardener ratio of 4 : 1 and was postcured.

Hardener H and hardener A were mixed with the epoxy resin at 4 : 1 and 3 : 1 resin-to-hardener ratios separately. A total of 80 g of the mixture was hand-laid in a mold with 8 cavities, each capable of holding 10 g of resin. The epoxy resin was cured for 24 h at 22°C according to the manufacturer's recommendation for initial curing. Half of the samples (two from each hardener set) were postcured for another 4 h at 100°C. All samples were left for a week before ToF-SIMS and contact-angle measurements were undertaken.

ToF-SIMS

ToF-SIMS was performed with a ToF-SIMS IV instrument (Ion-TOF GmbH, Germany) equipped

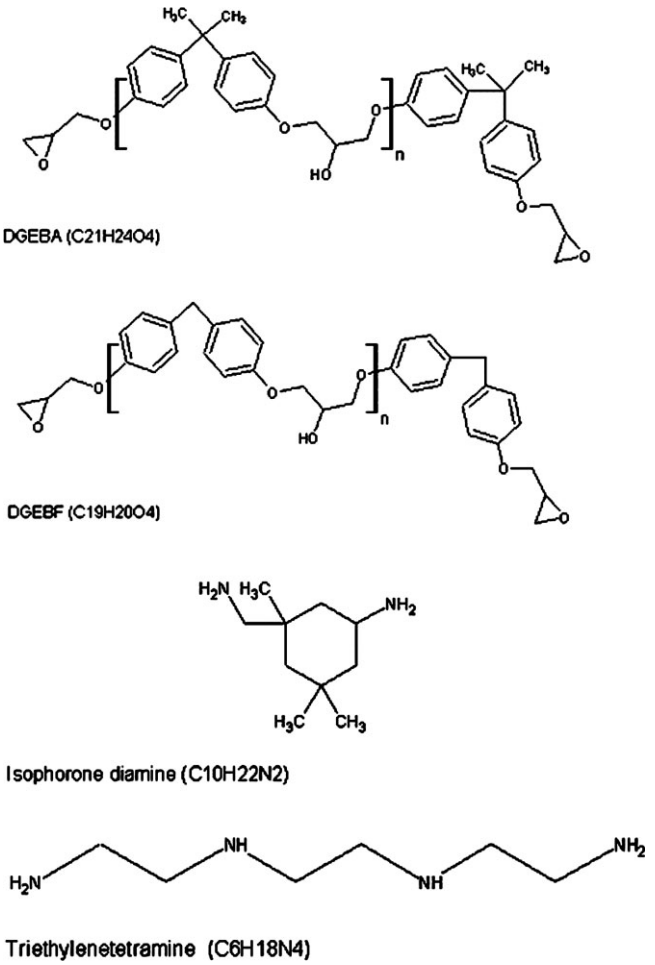

Figure 1 Molecular structures of (a) noncrosslinked poly-DGEBA ($C_{21}H_{24}O_4$; n = 0, 1,...), (b) DGEBF resin ($C_{19}H_{20}O_4$; n = 0, 1, ...), (c) IPD ($C_{10}H_{22}N_2$), and (d) Teta hardener ($C_6H_{18}N_4$).

with a reflectron time-of-flight mass analyzer, a Bi_3^+ ion gun (25 keV), and a pulsed electron flood source for charge compensation. The primary pulsed ion beam current was 1.1 pA, and the primary ion dose density was below the static secondary ion mass spectrometry limit of 10^{13} ions/cm^2. Positive high mass resolution (>7500 at $m/z = 29$) spectra were acquired from three separate 100 μm × 100 μm areas on each sample with a cycle time of 100 μs.

The peaks for ToF-SIMS data analysis were selected initially on the basis of reference libraries and previous assignments in the literature for DGEBA, DGEBF, IPD, Teta, and other amine molecules.[21–24] Further peaks were assigned with the library and the exact mass calculator tool in Ionspec software (Ion-TOF), including contaminant peaks, hydrocarbon peaks, and peaks likely to correspond to fragments of the resin/hardener that were not listed in the literature. All the significant peaks above the baseline in the m/z range of 0–350 were selected. The mass spectra were calibrated with a series of hydrocarbon (C_xH_y) peaks up to $m/z = 105$.

The data were grouped in a matrix, and the columns in the matrix were normalized to the total intensity. The matrix was mean-centered before PCA. PCA was performed with code developed in house that was based on the covariance method algorithm described in detail by Martens and Naes.[25]

Contact-angle measurements

Sessile drop contact-angle measurements for both precured and postcured epoxy resins were taken at room temperature with an OCA 20 optical contact-angle instrument (Dataphysics GmbH, Filderstadt, Germany). Milli-Q water (resistivity > 18.3 MΩ cm) and isopropyl alcohol were used as the nonpolar

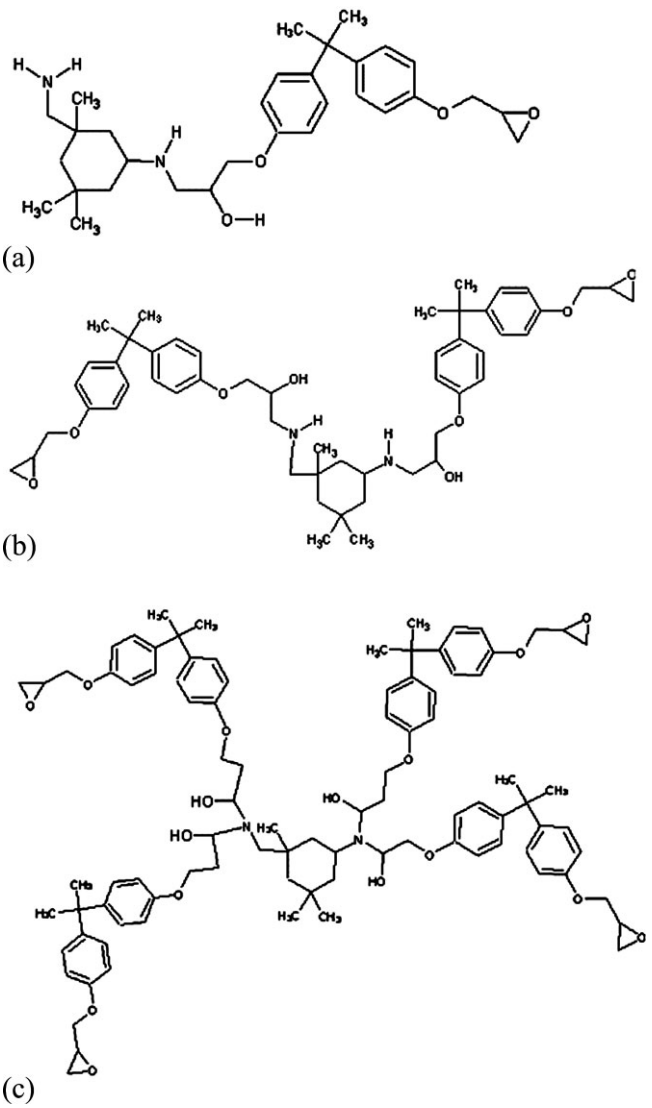

Figure 2 Structures produced by the epoxy resin curing reactions of DGEBA/IPD molecules: (a) blocking, (b) linear coupling, and (c) branching formation.

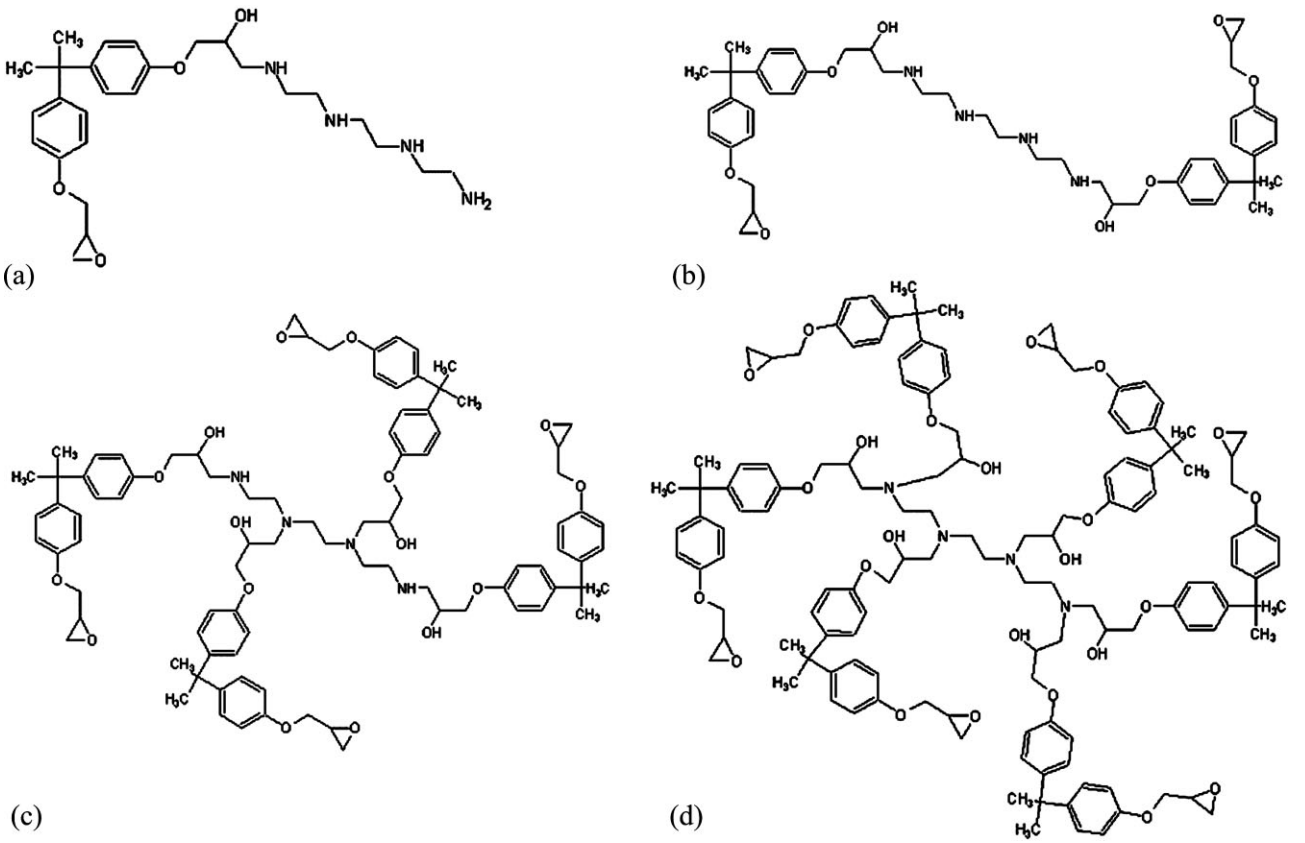

Figure 3 Structures produced by the epoxy resin curing reactions of DGEBA/Teta molecules: (a) blocking, (b) linear coupling, (c) partial branching, and (d) full branching formation.

and polar test liquids, respectively, with testing based on well-established methods reported in the literature.[10–12] The surface free energies of the epoxy resins were calculated with the Wu harmonic mean theory.[7,8] The contact-angle values were calculated from the mean of the left-hand and right-hand side contact angles of the sessile drop. This was repeated three times across the surface of each sample; average contact-angle values for each sample are reported.

RESULTS AND DISCUSSION

The stoichiometry information regarding the reactivity of the DGEBA-based epoxy resin with amine-type hardeners indicates that it progresses by the reaction of its epoxide groups through blocking, coupling, branching, and crosslinking bonding reactions with the amine groups.[17] Both IPD and Teta molecules couple with the epoxide group via the transformation of the hydrogen atom of the amine functionality. The IPD molecule has the potential to link four epoxy resin molecules, as shown in Figure 2. The Teta molecule, on the other hand, can link as many as six DGEBA or DGEBF molecules, and this provides up to 50% more linking opportunities than those achieved by the IPD molecule (Fig. 3). The crosslinking reaction progresses through the initial steps of coupling and branching reactions. The final network structure and density depend greatly on the conversion process of coupling and branching into crosslinking, which in turn depends on the overall curing reaction conditions.[17]

The surface energies calculated with the Wu harmonic mean theory from contact-angle measurements for cured and postcured epoxy resins cured by both hardeners (A and H) are presented in Table I. The epoxy resin cured with hardener H showed higher surface energy than the epoxy resin cured with hardener A among the cured and postcured samples, with the exception of sample A4P, which showed the highest surface energy value of all samples. The epoxy resin cured with hardener H showed significantly higher polar components than the epoxy resin cured with hardener A, with the exception of A4P. The dispersion components of the surface energy were not significantly different across the samples and were not affected significantly by the resin postcuring process. The polar components of the surface energy decreased for hardener H and increased for hardener A as a result of postcuring. All samples with a resin-to-hardener ratio of 3 : 1

TABLE I
Surface Energies of Epoxy Resins Measured with Contact-Angle Measurements and Calculated According to the Wu Harmonic Mean Theory

	Surface energy (mN/m)	Standard deviation	Dispersion	Polar
Cure only				
H3C	40.0	0.4	14.6	25.4
H4C	35.1	1.2	14.9	20.2
A3C	30.2	0.9	15.3	14.9
A4C	33.6	0.1	15.0	18.6
Postcure				
H3P	35.8	0.4	14.8	21.0
H4P	36.5	0.5	14.8	21.7
A3P	30.9	0.1	14.9	16.0
A4P	41.3	0.4	14.2	27.1

showed surface energies less than those of the samples with a resin-to-hardener ratio of 4 : 1, with the exception of sample H3C. The surface energies and adhesion strength have been reported to advance as the cured epoxy resin approaches the total conversion.[26,27] On the basis of the surface energy data reported in Table I, it is reasonable to assume that the epoxy resin cured with hardener H would have a higher curing conversion rate than that cured with hardener A. Furthermore, resin samples made with a resin-to-hardener ratio of 3 : 1 would achieve a higher curing conversion rate than 4 : 1 ratio samples with hardener H. A resin-to-hardener ratio of 4 : 1 would lead to a higher curing conversion rate than a 3 : 1 ratio with hardener A. Sample A4P was expected to achieve the highest curing conversion, whereas sample A3C showed the lowest curing conversion rate.

PCA was conducted initially with ToF-SIMS preprocessed positive data for all epoxy resin samples. The first (PC1), second (PC3), third (PC3), and fourth (PC4) principal components accounted for 53.9%, 18.8%, 17.6%, and 4.9% of the total variance captured by PCA, respectively. The remaining principal components accounted, in all, for no more than 4.8%, and hence they were neglected in the presentation of the results. Figure 4 shows the PCA score plots of the ToF-SIMS positive-ion spectra of all the samples. Figure 5 shows the PCA loading plots for the ToF-SIMS positive-ion spectra. Figure 6 shows the relative ion intensity of the ions that contributed most strongly to the PCA loadings.

Figure 4(a) shows the score plot for PC1 versus PC2 and indicates that the epoxy resin samples were separated largely in PC1 according to the network structure in the resin. Information collected by PC1 is related to the different reaction paths of the different hardeners used to cure the resin. Hardener A, which mainly consists of Teta molecules, generates more opportunities for reactions with the epoxide groups of the epoxy resin because of its multiple nitrogen reacting sites. Hardener H and its constituent IPD molecules generate fewer nitrogen reacting sites (Figs. 2 and 3). The effect of postcuring was not clearly indicated by PC1. PC1 is dominated by the strong variance related to the main chemical phenomena of the hardener/resin crosslinking network structure.

Figure 5(a) shows the loading plot for PC1. The main contributions in PC1 arise from the relative ion intensity of the aliphatic hydrocarbon ions $C_3H_5^+$, $C_5H_9^+$, $C_6H_9^+$, $C_4H_8^+$, and $C_3H_7^+$. The different reaction paths and functionalities of the Teta and IPD molecules are explained by PC1 loadings. Resin samples cured with hardener A showed higher PCA-identified aliphatic hydrocarbon ion intensities for $C_3H_5^+$, $C_4H_8^+$, and $C_5H_9^+$ than the resin samples cured with hardener H, as shown in Figure 6(a,b). The relative ion intensity of the aliphatic hydrocarbon ions in DGEBA/DGEBF molecules has been linked previously to the formation of large

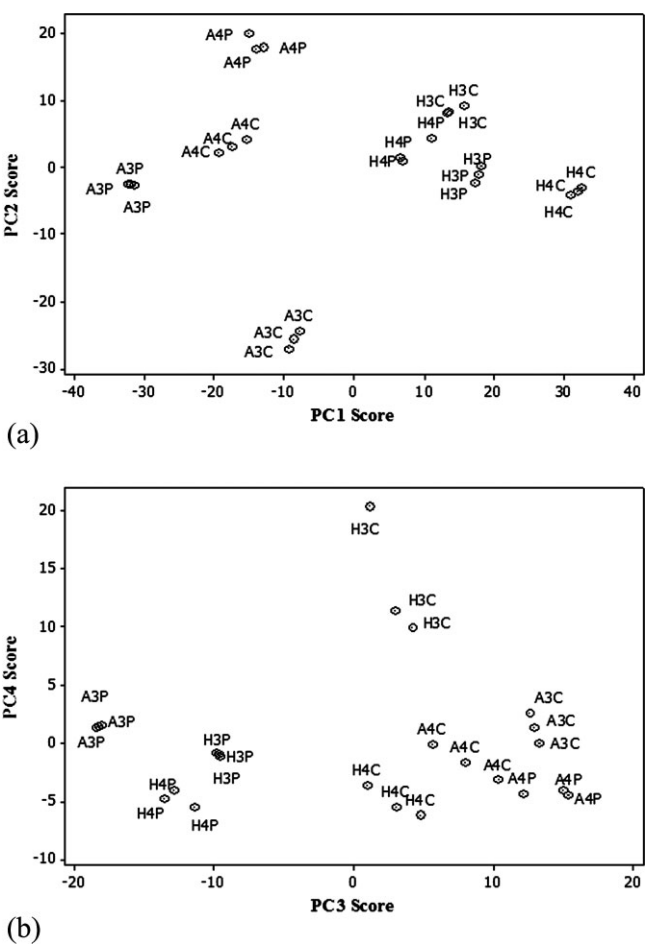

Figure 4 PCA score plots of positive ToF-SIMS spectra for (a) the PC1 score versus the PC2 score and (b) the PC3 score versus the PC4 score.

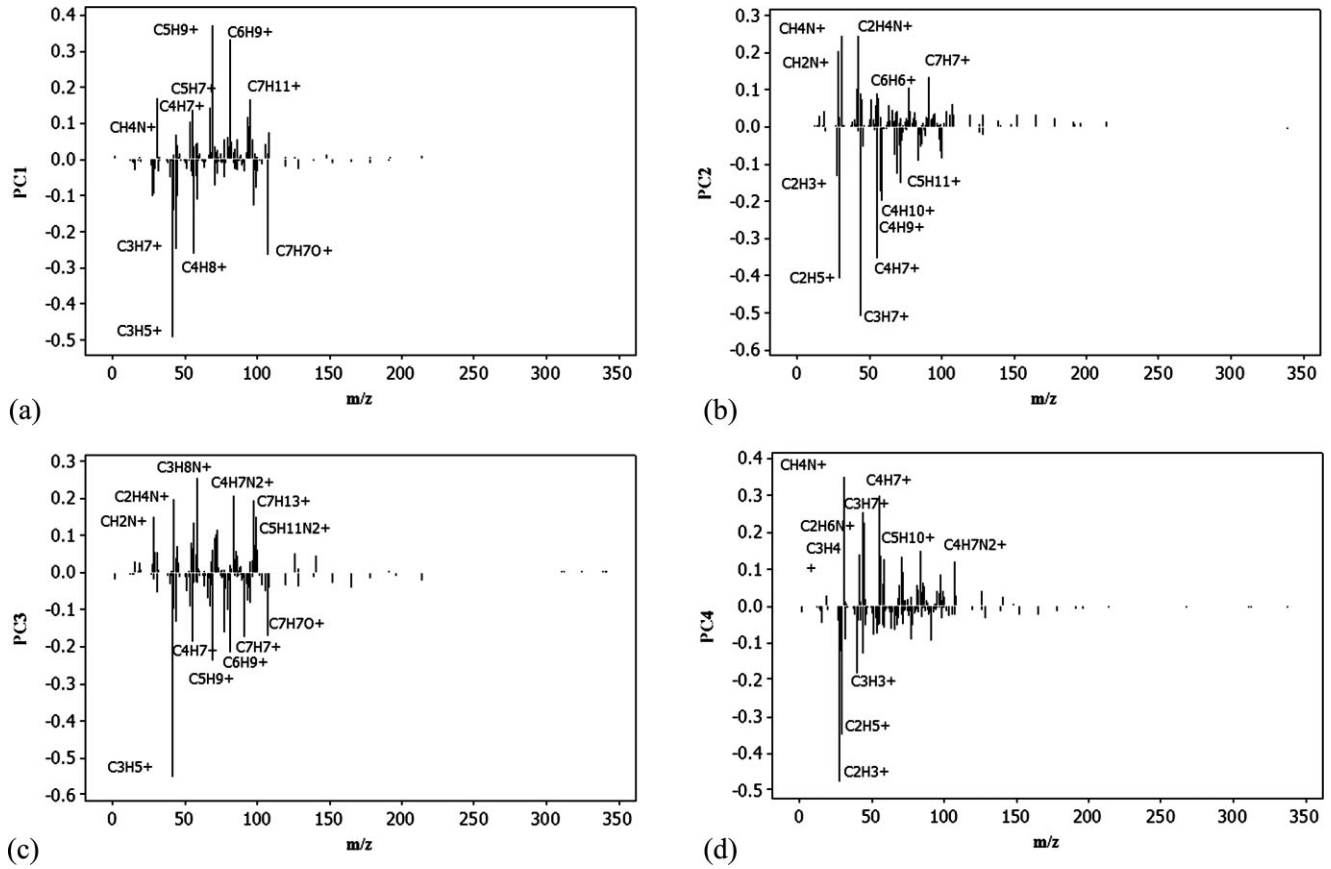

Figure 5 PCA loading plots for ToF-SIMS positive spectra of (a) PC1, (b) PC2, (c) PC3, and (d) PC4.

structured molecules.[17] The PC1 loadings indicate that the resin cured with hardener A generated more complex branching and denser networks than the resin samples cured with hardener H. Furthermore, the increased network density associated with postcuring was more evident in the resin cured with hardener A than in samples cured with hardener H, as evidenced by the ion intensities of $C_3H_5^+$, $C_4H_8^+$, and $C_5H_9^+$ [Fig. 6(a)].

Another significant contribution is related to the relative ion intensities of $C_7H_7O^+$ and CH_4N^+ ions. The concentration of the $C_7H_7O^+$ relative ion intensity in PC1 is related to the development of branching reactions and to the curing reaction conversion.[18] The relative ion intensity of $C_7H_7O^+$ initially increases with an increasing branching reaction rate and then decreases as the curing reaction conversion increases.[18] This is because the $C_7H_7O^+$ relative ion intensity increases in response to the easier and lower energy secondary ion fragmentation of the small coupling and branching structures and decreases as the larger crosslinking structures form, which require much more energy for ionization.[18,28] Figure 6(a) shows that the resin samples cured with hardener A, samples A3C and A4C, had higher relative ion intensities of the $C_7H_7O^+$ ion than other samples, indicating the presence of coupling and branching structures at a higher concentration than for the other samples. The $C_7H_7O^+$ ion intensity dropped for the postcured samples, A3P and A4P, as postcuring promoted crosslinking. This finding is in agreement with the stoichiometric assumption explained earlier (Fig. 3) and with the curing conversion assumption made on the basis of the surface energy measurements (Table I). The resin cured with hardener H showed chemical phenomena that were the opposite of those of the resin cured with hardener A. Branching reactions seemed to gain momentum over crosslinking during postcuring, as indicated by the increase in the $C_7H_7O^+$ relative ion intensity and as shown in Figure 6(a). This indicates chain scission in the resin cured with hardener H as a result of postcuring or coupling formation [Fig. 2(b)], and they transformed into branching [Fig. 2(c)] in the process.

According to the information collected by PC2, samples A3C and A4P were distinguished from other sample groups and appeared on the opposite side of the score plot in comparison with the other samples (which overlapped with one another). Table I shows that sample AC3 had the lowest surface energy, whereas sample A4P had the highest surface energy in the group. Hence, information collected in PC2 was sensitive to molecular changes related to

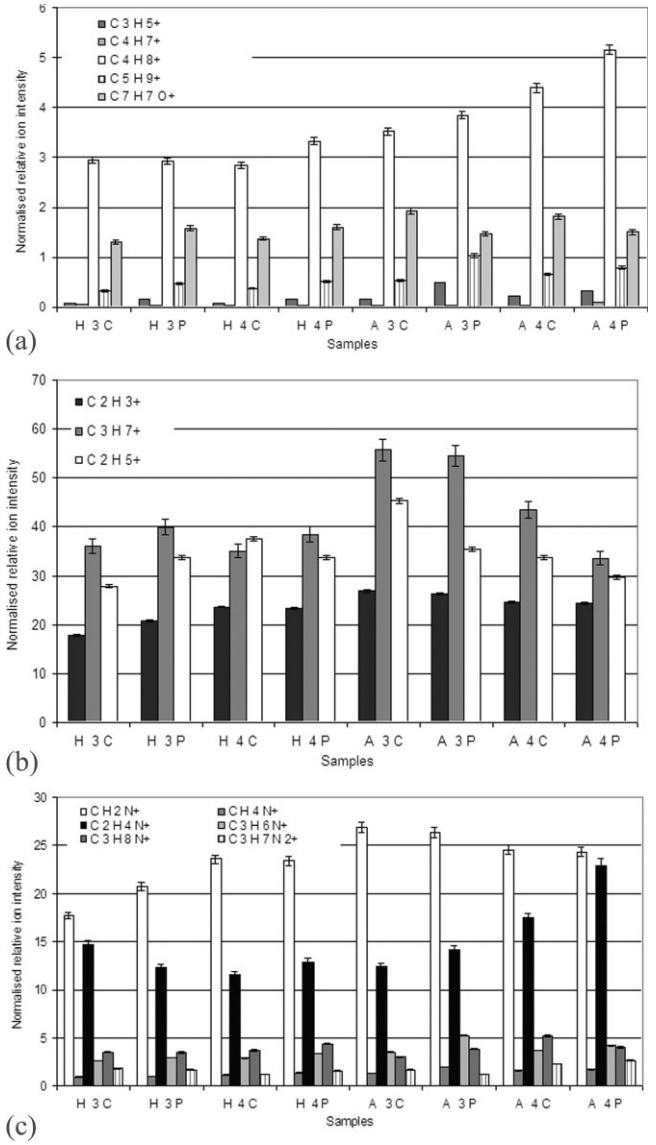

Figure 6 Variation in the intensity of secondary ion peaks of positive ToF-SIMS spectra that showed significant variance by PCA. Each bar represents the average of three readings of ion intensities with the standard deviation.

the surface energy of the cured and postcured epoxy resin samples. Epoxy resin samples cured with hardener A were more scattered than those cured with hardener H, with sample AC3 separated from the rest of the samples in both PC1 and PC2. This indicates that the molecular structure for the epoxy resin samples cured with hardener A was more strongly influenced by the resin-to-hardener ratio and the postcuring conditions than those cured with hardener H.

Figure 5(b) shows the loading plot for PC2. Aliphatic hydrocarbon ions are the highest contributors to PC2 via the molecular ions $C_3H_7^+$, $C_2H_5^+$, $C_4H_7^+$, $C_4H_9^+$, and $C_4H_{10}^+$. Shown on the opposite side of the loading plot is the contribution of the nitrogen-containing ions CH_4N^+, $C_2H_4N^+$, and CH_2N^+. There is also a contribution from $C_7H_7^+$ and $C_6H_6^+$, which occurs in the direction opposite of that of the other aliphatic hydrocarbon ions. PC2 captured information related to the largest difference in the surface energy among the samples. A comparison of the samples that had the lowest surface energy (A3C) and the highest surface energy (A4P), using Table I and Figures 4(a), 5(b), and 6, indicates multiple correlations. Higher surface energy is indicated by a significant increase in the relative intensity of the $C_2H_4N^+$ ion [Fig. 6(c)]. Higher surface energy is also correlated to a lower relative intensity of the $C_3H_7^+$ and $C_2H_5^+$ ions. The higher relative intensity of the $C_2H_4N^+$ ion indicates that the surface is rich with nitrogen-containing functional groups and hence more polar, and this may contribute to higher surface energy. The $C_3H_7^+$ and $C_2H_5^+$ ions may result from fragmentation of either DEGBA or Teta species (or both), so it is difficult to identify a trend that correlates with the surface energy.

Figure 4(b) shows the score plot for PC3 versus PC4. Sample H3C is shown as an outlier in PC4. The

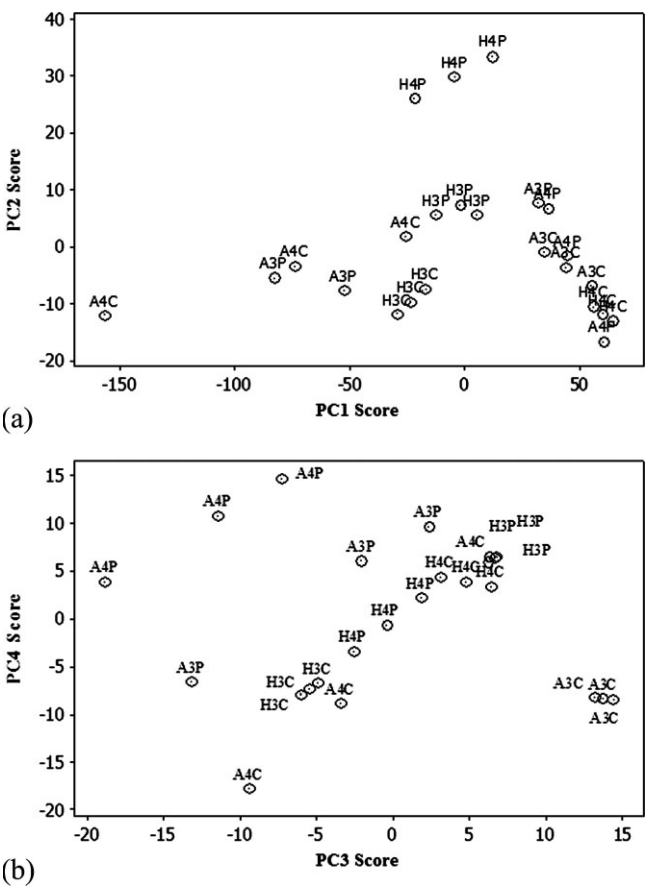

Figure 7 PCA score plots of negative ToF-SIMS spectra for (a) the PC1 score versus the PC2 score and (b) the PC3 score versus the PC4 score.

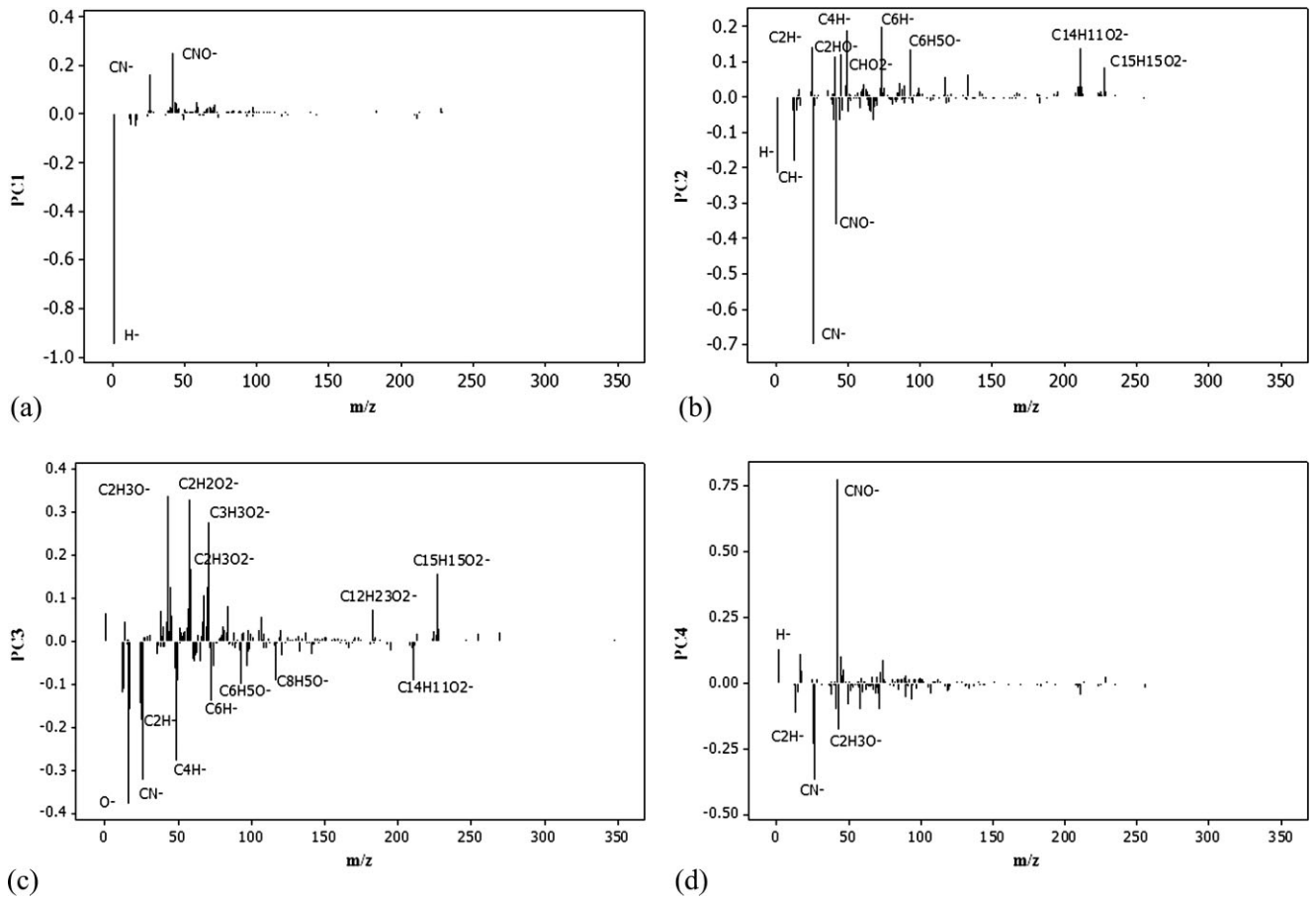

Figure 8 PCA loading plots for ToF-SIMS negative spectra of (a) PC1, (b) PC2, (c) PC3, and (d) PC4.

rest of the samples showed a trend in PC3 that almost separated the postcured samples from the cured sample, that is, with the exception of sample A4P, which is featured in the section on cured resins. This indicates a phenomenon that is related to the postcuring process, which applies to all samples except A4P. Figure 5(c) shows the loading plot for PC3. Aliphatic hydrocarbon ions are the highest contributors to PC3 and are represented by the ions of $C_3H_5^+$, $C_5H_9^+$, $C_6H_9^+$, $C_4H_7^+$, and $C_7H_7^+$. Shown on the opposite side of the loading plot is the significant contribution of the nitrogen-containing ions of $C_3H_8N^+$, $C_2H_4N^+$, $C_4H_7N_2^+$, CH_2N^+, and $C_5H_{11}N_2^+$. The fact that these different ion groups appear in opposite directions indicates that they are products of different reactions. These products are the hardener molecules represented by the $C_xH_yN_z^+$ ions through coupling and branching structures and the resin crosslinked network represented by the aliphatic hydrocarbon ions. The cured samples and sample A4P showed higher relative ion intensities of the $C_3H_7N_2^+$ ion and higher overall intensities for nitrogen-containing ions. There was also a contribution from the $C_7H_7O^+$ ion and the $C_7H_{13}^+$ ion, which appeared in the direction opposite of that of the other aliphatic hydrocarbon ions.

Figure 5(d) shows the loading plot for PC4. Major contributions to PC4 can be seen in the relative ion intensity of $C_2H_3^+$, $C_2H_5^+$, and $C_3H_3^+$ from one direction, whereas the other direction shows contributions from the CH_4N^+, $C_2H_6N^+$, $C_3H_7^+$, and $C_4H_7^+$ ions. A comparison of Figures 4(b), 5(d), and 6(b) shows that the H3C sample was separated from the rest of the samples because of the lower relative intensity of the $C_2H_3^+$ and $C_2H_5^+$ molecular ions, which possibly indicated a lower network density.[18] All other samples showed similar values.

As a result of PCA of the positive-ion ToF-SIMS spectra, multiple chemical and physical phenomena are revealed by the different principal components. PC1 collected information related to the curing reaction and network structure on the surface of the epoxy resin samples. It provided the means for identifying which of the two hardener systems produced a denser network. Furthermore, PC1 collected information regarding the effect of postcuring on the overall curing reaction conversion. PC2 collected information that provided correlations between the

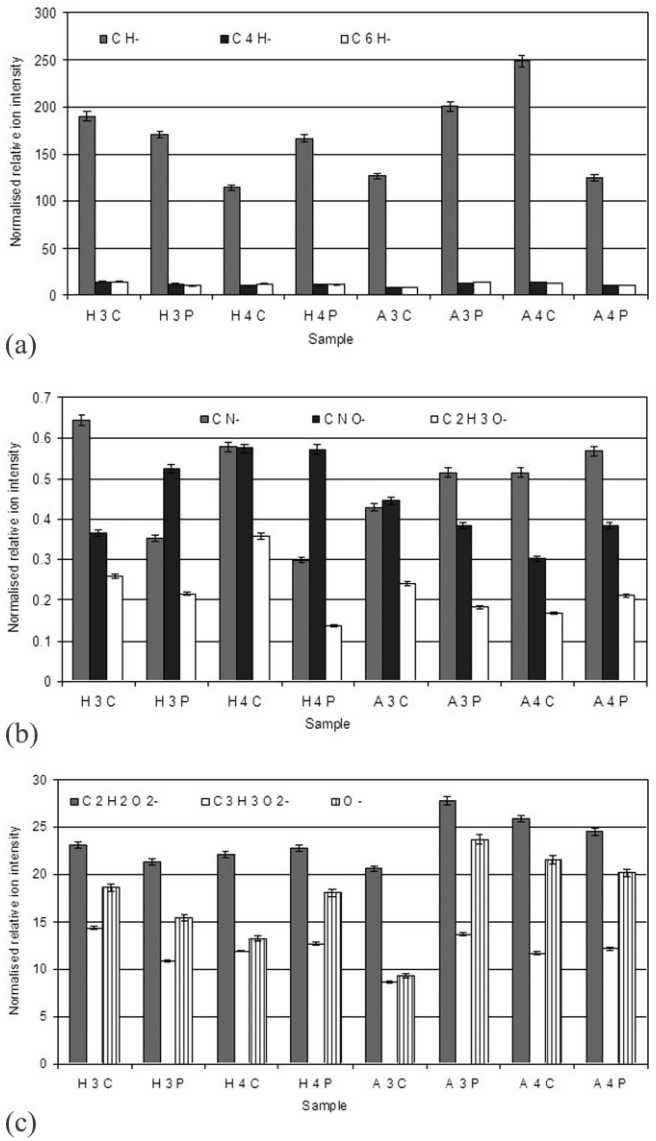

Figure 9 Variations in the intensity of secondary ion peaks of negative ToF-SIMS spectra that showed significant variance by PCA. Each bar represents the average of three readings of ion intersities with the standard deviations.

specific ion intensities and surface energy. PC3 and PC4 revealed the two dominant reaction pathways in the curing and postcuring reactions, that is, the consumption of the hardener molecules and the development of the crosslinking network, as the curing reaction progressed.

Figures 7 and 8 show the PCA scores and loading plots, respectively, of the negative ToF-SIMS spectra. The variance contributions of the principal components were 88.1% for PC1, 5.5% for PC2, 2.3% for PC3, and 2% for PC4. The remaining principal components accounted for less than 2.1% and were not included in the analysis. Information collected by the PC1 scores did not result in a clear trend, and all the samples overlapped another, as shown in Figure 7(a). A comparison with Figure 8(a) indicates that the major contributor to PC1 is the H^- ion, with less significant contributions from the CN^- and CNO^- ions. The H^- ion relative intensity results from multiple fragmentations of many larger molecular ions and surface constituents. The evolution of H^- ions in this instance provides little assistance in separating or grouping relevant chemical or physical phenomena.

PC2 scores separated the H4P sample from the rest of the samples, which overlapped one another, as shown in Figure 7(a). Figure 8(b) shows that the major contributors to PC2 are the CN^- and CNO^- ions. Further contributions with lesser significance come from the C_4H^-, C_2HO^-, CH^-, H^-, C_2H^-, C_6H^-, $C_6H_5O^-$, $C_{14}H_{11}O_2^-$, and $C_{15}H_{15}O_2^-$ ions. Sample H4P showed the lowest relative ion intensity of the CN^- ion in comparison with the other samples, as shown in Figure 9. As the curing reaction progressed for the resin samples reacted with hardener H, the ion intensity of IPD-related species started to decrease.[17] Hence, information in PC2 indicates that sample H4P achieved the highest curing reaction conversion in comparison with the other resin samples cured with hardener H. The resin samples cured with hardener A were likely to generate higher intensities for nitrogen-containing ions, even at the same conversion rate, because of the higher number of nitrogen atoms in the Teta molecule in comparison with the IPD molecule.

The PC3 score plot shown in Figure 7(b) separates sample A3C from the rest of the samples. All other samples overlapped and did not show a clear trend. The PC3 loading plot [Fig. 8(c)] shows numerous ions that contribute to the PC3 loadings, such as the O^-, CN^-, $C_2H_3O^-$, $C_2H_2O_2^-$, $C_3H_3O_2^-$, C_2H^-, C_4H^-, C_6H^-, $C_6H_5O^-$, $C_8H_5O^-$, $C_{15}H_{15}O_2^-$, $C_{12}H_{23}O_2^-$, and $C_4H_{11}O_2^-$ ions. Sample A3C showed the lowest relative ion intensity of the O^-, $C_2H_2O_2^-$, and $C_3H_3O_2^-$ ions in comparison with the other samples. That indicates lower surface polarity resulting in lower surface energy, which also agrees with the finding from Table I. Hence, PC3 collected information that was sensitive to the changes in the surface energy.

The PC4 score plot [Fig. 7(b)] shows a random distribution of samples. However, there is a cluster of samples appearing in both PC3 and PC4 that shows a trend which starts from sample H3C and increases with samples H4P, H4C, A4C, and H3P. The PC4 loading plot [Fig. 8(d)] shows that the main contribution comes from the CNO^- ion, whereas less significant contributions come from the CN^-, C_2H^-, and $C_2H_3O^-$ ions. There is significant residual noise in the loadings of PC4, mainly from the C_2H^- ion count, and this makes interpreting the data quite complex. The C_2H^- ion, in common with H^-, may originate from fragmentation of numerous secondary

ions or from different molecular structures in the final network.

CONCLUSIONS

Surface energy calculations showed that using different hardeners with different mixing ratios for curing epoxy resins resulted in different resin surface energies. Postcuring of the epoxy resin resulted in an increase in the polar components of the surface energy for Teta-molecule-based hardener A and a decrease in the resin samples that were cured with IPD-based hardener H.

ToF-SIMS generated a broad range of information revealing the reaction steps, path, and mechanism for the epoxy resin cured with IPD- and Teta-based hardeners. PCA of positive- and negative-ion ToF-SIMS data provided insight into the molecular characteristics of the cured and postcured epoxy resin resulting from the use of different hardeners, mixing ratios, and postcuring. The effect of the surface structure on the surface energy was also explained. PCA of the positive spectra showed that the branching, network density, and curing and postcuring conversion rates could be identified as separate phenomena. Through the changes of the aliphatic hydrocarbon ions, a denser network was achieved from reacting the epoxy resin with hardener A. However, the resin cured with hardener A also showed a high degree of branching structures, as indicated by the higher relative ion intensity of the $C_7H_7O^+$ ion. Postcuring resulted in the reduction of the relative ion intensity of the $C_7H_7O^+$ ion, which meant the development of the branching formation into the crosslinking formation.

It was found that samples with higher relative ion intensities of the $C_xH_yN_z^+$ ion groups tended to give rise to higher surface energies. PCA also enabled the detection of the curing reaction steps of coupling and branching from one side and crosslinking reactions from the other side. The success of coupling and branching reactions gave rise to the relative ion intensity of the $C_xH_yN_z^+$ ion counts, whereas the crosslinking reaction step gave rise to the aliphatic hydrocarbon ion counts. PCA of the negative spectra shed some light on the different conversion rates among the samples, which were indicated by the different relative ion intensities of the CN^- and CNO^- ions. Also, correlations were established between the surface energy and the presence of the O^-, $C_2H_2O_2^-$, and $C_3H_3O_2^-$ ions.

References

1. Han, J. H.; Kim, C. G. Compos Struct 2006, 72, 218.
2. Williams, G.; Trask, R.; Bond, I. Compos A 2007, 38, 1525.
3. Penn, L. S.; Wang, H. In Handbook of Composites; Peters, S. T., Ed.; Chapman & Hall: London, 1998.
4. Ramírez, C.; Rico, M.; López, J.; Montero, B. J Appl Polym Sci 2007, 103, 1759.
5. Lahlali, D.; Naffakh, M.; Dumon, M. Polym Eng Sci 2005, 45, 1582.
6. Lee, Y. K.; Kim, H. J.; Rafailovich, M.; Sokolov, J. Int J Adhes Adhes 2002, 22, 375.
7. Chiu, S. M.; Hwang, S. J.; Chu, C. W.; Gan, D. Thin Solid Films 2006, 515, 285.
8. Owens, D. K.; Wendt, R. C. J Appl Polym Sci 1969, 13, 1741.
9. Clint, J. H. Curr Opin Colloids 2001, 6, 28.
10. Neumann, A. W.; Spelt, J. Applied Surface Thermodynamics; Marcel Dekker: New York, 1996.
11. Tavana, H.; Neumann, A. W. Adv Colloid Interface 2007, 132, 1.
12. Della Volpe, C.; Maniglio, D.; Brugnara, M.; Siboni, S.; Morra, M. J Colloid Interface Sci 2004, 271, 434.
13. Lim, K. B.; Lee, B. S.; Kim, J. T.; Lee, D. C. Surf Interface Anal 2002, 33, 918.
14. Wang, J. Microelectron Reliab 2002, 42, 293.
15. Hartwig, A.; Vit, G.; Dieckhoff, S.; Hennemann, O. D. Angew Makromol Chem 1996, 238, 177.
16. Abbasian, A.; Ghaffarian, S. R.; Mohammadi, N.; Fallahi, D. Colloids Surf A 2004, 236, 133.
17. Awaja, F.; van Riessen, G.; Fox, B.; Kelly, G.; Pigram, P. J. J Appl Polym Sci 2009, 113, 2765.
18. Awaja, F.; van Riessen, G.; Fox, B.; Kelly, G.; Pigram, P. J. J Appl Polym Sci 2008, 110, 2711.
19. Wagner, M. S.; Graham, D. J.; Ratner, B. D.; Castner, D. G. Surf Sci 2004, 570, 78.
20. Graham, D. J.; Wagner, M. S.; Castner, D. G. Appl Surf Sci 2006, 252, 6860.
21. Coullerez, G.; Leonard, D.; Lundmark, S.; Mathieu, H. J Surf Interface Anal 2000, 29, 431.
22. Rattana, A.; Abel, M. L.; Watts, J. F. Int J Adhes Adhes 2006, 26, 28.
23. Treverton, J. A.; Paul, A. J.; Vickerman, J. C. Surf Interface Anal 1993, 30, 449.
24. Woerdeman, D. L.; Parnas, R. S.; Giunta, R. K.; Wilkerson, A. L. J Colloid Interface Sci 2002, 249, 246.
25. Martens, H.; Naes, T. Multivariate Calibration; Wiley: London, 1989.
26. Lee, J. R.; Park, S. J.; Seo, M. K.; Baik, Y. K.; Lee, S. K. Nucl Eng Des 2006, 236, 931.
27. Page, S. A.; Mezzenga, R.; Boogh, L.; Berg, J. C.; Manson, J. E J Colloid Interface Sci 2000, 222, 55.
28. Leggett, G. J. In Wiley Static SIMS Library; Vickerman, J. C.; Briggs, D.; Henderson, A., Eds.; Surface Spectra: Manchester, United Kingdom, 1998; p 19.